Corresponding Author

Shinobu Satoh

Graduate School of Life and Environmental Sciences, University of Tsukuba, Tsukuba, Ibaraki, 305-8572, Japan

Phone. +81-29-853-4672

Fax, +81-29-853-4579.

E-mail: satoh.shinobu.ga@u.tsukuba.ac.jp

Member of the Botanical Society of Japan

Subject Areas

1. Genetics/Developmental Biology

Number of black-and-white figures, color figures, and tables

Black-and-white figures: 3

Color figures: 3

Tables: 3

Title

Expression and functions of *Myo*-inositol monophosphatase family genes in seed development of *Arabidopsis*

Authors

Yuko Sato

Graduate School of Life and Environmental Sciences, University of Tsukuba, Tsukuba, Ibaraki, 305-8572, Japan

e-mail: s0530456@yahoo.co.jp

Katsumi Yazawa

National Institute of Agrobiological Science, 2-1-2 Kannondai, Tsukuba, Ibaraki 305-8602, Japan

e-mail: kyazawa@affrc.go.jp

Seiji Yoshida

National Institute for Environmental Studies, Tsukuba, Ibaraki, 305-0053, Japan

e-mail: YOSHIDAS2@nittobogrp.com

Masanori Tamaoki

National Institute for Environmental Studies, Tsukuba, Ibaraki, 305-0053, Japan

e-mail: mtamaoki@nies.go.jp

Nobuyoshi Nakajima

National Institute for Environmental Studies, Tsukuba, Ibaraki, 305-0053, Japan

e-mail: naka-320@nies.go.jp

Hiroaki Iwai

Graduate School of Life and Environmental Sciences, University of Tsukuba, Tsukuba, Ibaraki, 305-8572, Japan

E-mail: hiroiwai@sakura.cc.tsukuba.ac.jp

Tadashi Ishii

Forestry and Forest Products Research Institute, Tsukuba, Ibaraki, 305-8687, Japan

e-mail: tishii@ffpri.affrc.go.jp

Shinobu Satoh

Graduate School of Life and Environmental Sciences, University of Tsukuba, Tsukuba, Ibaraki, 305-8572, Japan

E-mail: satoh.shinobu.ga@u.tsukuba.ac.jp

Abstract

Myo-inositol monophosphatase (IMP) catalyzes the dephosphorylation of *myo*-inositol 3-phosphate in the last step of *myo*-inositol biosynthesis. IMP is also important in phosphate metabolism and is required for the biosynthesis of cell wall polysaccharides, phytic acid, and phosphatidylinositol. In *Arabidopsis*, IMP is encoded by *VTC4*. There are, however, two additional IMP candidate genes, *IMPL1* and *IMPL2*, which have not yet been elucidated. In our genetic studies of *Arabidopsis* IMP genes, only the loss-of-function mutant *impl2* showed embryonic lethality at the globular stage. All IMP genes were expressed in a similar manner both in the vegetative and reproductive organs. In developing seeds, expression of IMP genes was not coupled with the expression of the genes encoding *myo*-inositol phosphate synthases (MIPSs), which supply the substrate for IMPs in the *de novo* synthesis pathway. Instead, expression of IMP genes was correlated with expression of the gene for *myo*-inositol polyphosphate 1-phosphatase (*SAL1*), which is involved in the *myo*-inositol salvage pathway, suggesting a possible salvage pathway role in seed development. Moreover, the partial rescue of the *impl2* phenotype by histidine application implies that *IMPL2* is also involved in histidine biosynthesis during embryo development.

Key words: *Arabidopsis thaliana* · Embryogenesis · Gene expression · Histidine · *IMPL2* ·

Myo-inositol.

Introduction

In eukaryotes, *myo*-inositol is a key precursor to various phospho metabolites such as phytic acid, phosphatidylinositol, Indole-3-acetic acid conjugate of *myo*-inositol, and cell wall polysaccharides (Loewus and Murthy 2000). *Myo*-inositol is synthesized *de novo* from glucose 6-phosphate in two sequential steps catalyzed by *myo*-inositol phosphate synthase (MIPS) and *myo*-inositol monophosphatase (IMP). IMP has been purified from rat (Takimoto et al. 1985), bovine (Gee et al. 1988; Diehl et al. 1990), and human (McAllister et al. 1992; Ohnishi et al. 2007) brains. Mammalian IMP requires Mg^{2+} for its activity and is inhibited by Li^{+}, Ca^{2+}, and Mn^{2+} (Hallcher and Sherman 1980; Loewus and Loewus 1983).

In many plant species, *MIPS1*, *MIPS2*, and *MIPS3* encode *myo*-inositol 3-phosphate synthase, which catalyzes the conversion of D-glucose 6-phosphate to *myo*-inositol 3-phosphate in the *de novo myo*-inositol synthesis pathway (Abid et al. 2009), and IMP catalyzes the last step of the conversion of glucose 6-phosphate to *myo*-inositol in tomato (Gillaspy et al. 1995; Styer et al. 2004), barley (Fu et al. 2008), soybean (Islas-Flores and Villanueva 2007), rice (Suzuki et al. 2007), and kiwifruit (Laing et al. 2004). RNAi suppression of *MIPS* activity in potato (*Solanum tuberosum*) results in a variety of morphological changes (Keller et al. 1998; Abid et al. 2009). The knockout of soybean *MIPS* (*GmMIPS*) leads to aborted seed development (Nunes et al. 2006; Abid et al. 2009). The MIPS enzymes are localized in both the cytosol and

chloroplast in higher organisms (Abid et al. 2009), and MIPS protein localizes to the cytosol of the *Arabidopsis* seed endosperm (Mitsuhashi et al. 2008).

Like animal IMPs, plant IMPs show Li^+ sensitivity (Hallcher and Sherman 1980; Loewus and Loewus 1983). An alternative pathway, called a salvage pathway, has been characterized in plants. In this pathway, *myo*-inositol is regenerated from various *myo*-inositol phosphate derivatives by dephosphorylation, and IMP is also responsible for the dephosphorylation of D-*myo*-inositol 4-phosphate, which is produced by SAL1 in the salvage pathway (Gillaspy et al. 1995; Quintero et al. 1996).

In *Arabidopsis*, VTC4, which exhibits IMP activity, also hydrolyzes L-galactose 1-phosphate (Torabinejad et al. 2009), as demonstrated in kiwifruits (Laing et al. 2004). Thus, plant IMPs appear to have broad substrate specificity. In addition to *VTC4*, *Arabidopsis* databases indicate that *IMPL1* and *IMPL2* are putative IMPs (Laing et al. 2004; Conklin et al. 2006; Torabinejad et al. 2009). In this study, histological analysis and real-time PCR of *VTC4*, *IMPL1*, and *IMPL2* showed similar organ expression patterns at different developmental stages. Their expression patterns were correlated with that of the *myo*-inositol polyphosphate 1-phosphatase gene, which is involved in the *myo*-inositol salvage pathway, rather than with those of the *myo*-inositol phosphate synthase genes involved in the *de novo* synthesis pathway. Moreover, only the *IMPL2* knockout line was lethal at the globular stage of embryogenesis and

could be complemented with a full-length *IMPL2*, suggesting that IMPL2 has another enzyme activity with critical roles in embryogenesis that is distinct from those of VTC4 and IMPL1.

Materials and methods

Plant materials and growth conditions

Seed stocks for SALK_124820 (*vtc4*), SALK_076930 (*impl2*) T-DNA insertion lines were obtained from the Arabidopsis Biological Resource Center at Ohio State University. *Arabidopsis thaliana* (ecotype Columbia-0) and the mutants were surface-sterilized and grown from seeds at 22°C under continuous illumination from white fluorescent tubes (32 μmol m^{-2} s^{-1}). To screen mutants, seeds were grown on medium containing 1.5% (w/v) purified agar supplemented with 0.5% (w/v) sucrose and 1/2 macro MS salts (Murashige and Skoog 1962). Plants grown in soil (Kureha Chemical Industry, Tokyo, Japan) were also illuminated (32 μmol m^{-2} s^{-1}) continuously at 22°C.

Microscopic observation of *Arabidopsis* embryos

Whole siliques of wild-type and heterozygous mutants were fixed in 90% (v/v) ethanol and 10% (v/v) acetic acid for over 1 h, washed with a graded ethanol series (90%, 70%, 50%, and 30% ethanol) for 20 min each, and cleared in chloral hydrate solution (8 g chloral hydrate/1 mL

glycerol/2 mL water) for 2–24 h at 4°C. Cleared seeds were observed under a stereomicroscope (CLS 150XB; Leica, Wetzlar, Germany) or a light microscope (DMRB; Leica). Embryos were observed using differential interference contrast imaging.

Isolation of T-DNA insertion mutants and complementation

Heterozygous plants were identified using gene-specific primers and a T-DNA left-border primer (LBb1) from the SIGnAL iSect Primer Design program at http://signal.salk.edu/. The gene-specific primers used for PCR were 5'-AATGTTAGCTCAGTCGCACTTCTTC-3' (S1) and 5'-GGTCAATGGACGCAAACTTACAA-3' (AS1). For complementation of *impl2*, the 4541-bp fragment, including the *IMPL2* promoter region and the full-length *IMPL2* gene, was amplified from *Arabidopsis* genomic DNA using the primers 5'-GATGGATTTGAAAGCGAGACACA-3' and 5'-ACACAAAGCCAAAAATAAAATAACTCTG-3', digested with *Bam*HI, and cloned into the binary cloning vector pPZP221 (Hajdukiewicz et al. 1994). The construct was transformed into heterozygous *impl2* plants with the *Agrobacterium*-mediated floral-dip method (Clough and Bent 1998), and the transgenic (T_1) plants were selected on agar plates supplemented with 50 μg mL^{-1} gentamycin. The T_2 seeds obtained from the gentamycin-resistant T_1 plants were grown in soil and subjected to PCR analysis using LBb1, gene-specific primers, and gentamycin primers

5’-TGGCGGTACTTGGGTCGATA-3’ (Gm-S1) and 5’-AGCAACGATGTTACGCAGCAG-3’ (Gm-AS1).

Construction of promoter-GUS and GUS activity assay

For the construction of the *VTC4* promoter–β-glucuronidase (GUS) gene fusion (*pVTC4::GUS*), a 1072-bp fragment upstream of the start codon was amplified by PCR from *Arabidopsis* genomic DNA using the primers 5’-GTCATCGCTGTCTTGGAACGAGAGAAAGGT-3’ and 5’-GAGTGATGCTTTCTTTACTTTGGGATGTGTTTCAG-3’. For the construction of the *IMPL1* promoter–*GUS* fusion (*pIMPL1::GUS*), a 300-bp fragment upstream of the start codon and a 1237-bp downstream fragment including introns and exons were amplified by PCR from *Arabidopsis* genomic DNA using the primers 5’-ACTGTATCTTCCCGGTATGATCTCC-3’ and 5’-ATGAATTTTTTGCCCGTTACACA-3’.

For the construction of the *IMPL2* promoter–*GUS* fusion (*pIMPL2::GUS*), an 800-bp fragment upstream of the start codon and a 900-bp downstream fragment including introns and exons were amplified by PCR from *Arabidopsis* genomic DNA using the primers 5’-TCCCACGACCCTCTTCAAGAC-3’ and 5’-GTCTGCAGATTCCTCTTTGCATCT-3’. These fragments were individually cloned into a pBI101 vector (Jefferson et al. 1987) with *Bam*HI sites, leading to a fusion between the promoter and *GUS*. The constructs were

individually transformed into *Arabidopsis* (Columbia-0) plants using the Agrobacterium-mediated floral-dip method, and the transgenic (T_1) plants were selected on agar plates supplemented with 50 μg mL^{-1} kanamycin.

Histochemical analysis was performed using GUS activity staining. The transformed plants were incubated for 2-8 h with X-Gluc solution (0.5 mg mL^{-1} 5-bromo-4-chloro-3-indolyl-β-D-glucuronide in 100 mM sodium phosphate buffer [pH 7.0] with 0.1% [v/v] Triton X-100, 1 mM potassium ferricyanide, and potassium ferrocyanide) at 37℃. The samples were then cleared with chloral hydrate solution for embryo analysis and observed under a light microscope (DMRB; Leica).

Quantitative real-time PCR

Plants were grown in soil. Rosettes and roots (3 wk after sowing), stems and cauline leaves (4 wk after sowing), and flower buds and siliques (4–12 d after flowering [DAF]) were collected from 10–15 plants for one experiment. Total RNA was extracted using both a Plant RNA Isolation Aid and an RNAqueous RNA isolation kit (Ambion, Austin, TX). First-strand cDNA was synthesized from total RNA (1 μg) with the QuantiTect Reverse Transcription kit (Qiagen, Valencia, CA). Quantitative real-time PCR with 2× SYBR Green Master Mix reagent (Qiagen) was performed using the first-strand cDNA as a template on a sequence detector system (ABI

Prism 7300; Applied Biosystems, Foster City, CA). The results were normalized using 18S rRNA as an internal control, and plasmid DNAs containing corresponding cDNAs were used as templates to generate a calibration curve. The experiments were repeated twice with similar results.

The primer sets used for PCR were as follows: 5'-TCCGGTAAAGATTTGGACATAACA-3' and 5'-CGCCTCAGCGAATAACTCCTT-3' for *VTC4*; 5'-CAATTTCAGGCCGGACAGTGAAC-3' and 5'-TCGCGTCTGATCAGAAACCTCAGA-3' for *IMPL1*; 5'-TGCCTGACTATGGCTTCAAACTCAA-3' and 5'-TACTTTCTGATAACCTCGCCGGAAG-3' for *IMPL2*; 5'-AAAGTTGAGAGCCCGAACGTGAAG-3' and 5'-AATCCATTGGTAAGTGCCATTGACG-3' for *MIPS1*; 5'-CATCGAGAGCTTCAAAGTAGAGAGTCCA-3' and 5'-CGACCCATTGATATGTACCGTTACGA-3' for *MIPS2*; 5'-GTTCATCGAAAGCTTCAAGGTTGAATC-3' and 5'-AGTCCATTGAAAAGCACCGTTTTTG-3' for *MIPS3*; and 5'-TCCAGCTCCATTGCCAATAAA-3' and 5'-AAAGCTCCATACTTTGCTTGGCTAT-3' for *SAL1*. The thermal cycle used was as follows: 95°C for 10 min, 40 cycles at 95°C for 15 s and 60°C for 1 min.

Histidine application

The method of histidine rescue was based on Muralla et al. (2007). Before plants began to bolt, 500 μM L-histidine (Product H8125; Sigma) was applied by daily watering to their roots. The wild-type and heterozygous plants were identified by PCR screening, and seeds of four siliques from a primary flowering stem on each of three wild-type and heterozygous plants were counted ~10 DAF.

Results

IMP genes have similar organ-dependent expression patterns, with the exception of *MIPS3*

To examine the tissue-specific expression patterns of IMP genes, *GUS* was fused to the promoter region of each gene and introduced into *Arabidopsis*. GUS activity was detected in whole plants at 5 (Fig. 1a, c, e) and 10 (Fig. 1b, d, f) d after sowing. *VTC4* GUS expression was the most remarkable, and was particularly strong in photosynthetic tissues (Fig. 1a, b). *IMPL1* GUS expression was observed in all tissues (Fig. 1c, d). *IMPL2* GUS expression was comparatively strong in roots, but had little hypocotyl expression (Fig. 1e, f).

Expression of *VTC4*, *IMPL1*, and *IMPL2* during plant development was investigated by quantitative PCR. Total RNA was extracted from rosette leaves and roots 3 wk after sowing and

from flowering stems and cauline leaves 4 wk after sowing, and the expression of genes related to *myo*-inositol biosynthesis was analyzed. mRNA levels for *IMPL1*, *IMPL2*, and *VTC4* were highest in rosette leaves and lowest in roots, and all three genes were similarly expressed (Fig. 2a). Gene expression levels were as follows: *VTC4* > *IMPL1* > *IMPL2*; the expression ratio in the root was the lowest in *IMPL1* but higher in *IMPL2* (Fig. 2a).

SAL1 (At5g63980), *MIPS1* (At4g39800), and *MIPS2* (At2g22240) (annotated in The *Arabidopsis* Information Resource [TAIR]), were similarly expressed as compared with *IMPL1*, *IMPL2*, and *VTC4*, but the expression of *MIPS2* in cauline leaves was remarkably low (Fig. 2b). Only *MIPS3* (At5g10170) showed a different pattern of expression among these genes, with the highest expression in the roots and low stem expression (Fig. 2b).

During seed development, the expression patterns of IMP genes are similar to that of SAL1 but not that of MIPS

To investigate the tissue-specific expression of IMP genes in reproductive organs, we performed a promoter-GUS assay on flowers and developing seeds. GUS activity was detected in the endosperm and in globular to heart stage embryos in the early stages of seed development, with no significant difference between *VTC4*, *IMPL1*, and *IMPL2* (Fig. 3a, d, g). In the torpedo stage, weak GUS staining was observed throughout the embryos of *pIMPL1*::*GUS* and *pIMPL2*::*GUS*,

and in the root of *pVTC4*::*GUS* (Fig. 3b, e, h). Dense GUS staining was observed in the pistil in all three transformants, and weak staining was also observed in the filament of *pIMPL1*::*GUS* (Fig. 3c, f, i). These results support the hypothesis that these genes play roles in seed development.

For the quantitative analysis, total RNA was extracted from whole siliques 4–12 DAF, and the expression was analyzed for seven genes related to *myo*-inositol biosynthesis. mRNA levels for the three IMP genes were highest at 4 DAF and then decreased until 12 DAF (Fig. 4a). The expression pattern of *SAL1* was similar way to those of the IMP genes, but the expression patterns of the three MIPS genes were different from those of the IMP genes and *SAL1* (Fig. 4b). *MIPS1* expression was high from 4 to 12 DAF, *MIPS2* was expressed consistently in flower buds and in siliques to 12 DAF, and *MIPS3* expression was high in flower buds and in siliques to 4 DAF and decreased thereafter until 12 DAF (Fig. 4b).

Only the *impl2* mutant has an embryo lethal phenotype in the IMP family

In *Arabidopsis*, VTC4 (At3g02870), IMPL1 (At1g31190), and IMPL2 (At4g39120) have sequence similarities to human IMP. To elucidate the functions of the IMP family in *Arabidopsis*, we obtained a T-DNA tag line for *VTC4* (SALK_124820), which showed unchanged and slightly reduced levels of ascorbic acid and *myo*-inositol, respectively, without altering plant

development (data not shown). Because no SALK lines for *IMPL1* were available, we suppressed the *IMPL1* gene by RNA-induced silencing. In plants grown under normal growth conditions, we did not find a significant developmental defect in *IMPL1*-RNAi transformants, which had about 55–70% inhibited gene expression (data not shown). Next, we attempted to clarify the biological functions of *IMPL2*. We obtained an *IMPL2* T-DNA insertion line (SALK_076930) from the SALK collections. Sequence analysis showed that the location of the T-DNA insertion was at the border of the first intron and the second exon of At4g39120, 506 bp downstream from the ATG initiation codon (Fig. 5).

Using a gene-specific PCR method, we verified that all the tested plants that had germinated from the seeds of the heterozygous *impl2* plants were wild type or heterozygous, indicating that homozygous plants were lethal. We used microscopy to observe seed maturation in the siliques of heterozygous plants. Compared with the wild-type plants, heterozygous plants had some abnormally shaped, white- or brown-colored small seeds (Fig. 6a, b). The ratio of normal to abnormal seeds in the siliques of the heterozygous plants was nearly 3:1 (Table 1). In the *impl2* mutant, embryo development was aborted in the early globular stage (Fig. 6c). To investigate whether this phenotype was due to the deficiency of *IMPL2*, we transformed the *impl2* heterozygous plants with a genomic fragment including full-length *IMPL2*. The gentamycin-resistant T_2 plants were selected, subjected to PCR analysis (Fig. 6d), and observed

microscopically. The resultant transformants did not exhibit the mutant phenotype, indicating that embryo lethality was due to deficient *IMPL2* function (Fig. 6e, Table 1).

The *impl2* mutant was partially rescued by histidine application

Because knockout of *IMPL2* resulted in an embryo-defective phenotype, we assumed that *IMPL2* has a unique additional function compared to IMP. One notable suggestion by Mormann et al. (2006) is that the *Corynebacterium glutamicum cg0910,* which has a high degree of sequence similarity to IMPs, encodes L-histidinol-phosphate phosphatase. In *Arabidopsis*, the knockout mutant of histidine biosynthesis genes (*HISN*) exhibited an embryo-defective phenotype (Stepansky et al. 2006; Muralla et al. 2007). Therefore, we hypothesized that *IMPL2* participates in histidine biosynthesis and that inhibition of histidine biosynthesis in the *impl2* mutant may result in embryonic lethality. To test this hypothesis, we performed a seed rescue test by giving histidine to heterozygous plants. The *impl2* plants were supplied with 1 mM histidine by watering daily beginning at 2-3 days before bolting, and normal and aborted seeds were counted after seed maturation (Muralla et al. 2007). We could not confirm the recovery from aborted to normal seeds by the application of 1 mM histidine in our experiment, but the heterozygous lines supplied with 500 μM histidine displayed a decrease in the number of aborted seeds compared with the control heterozygous *impl2* plants (Table 2). This result

implies that *IMPL2* also plays a role in histidine biosynthesis.

Discussion

In this study, we showed that homozygous *impl2* is embryonic lethal, although a similar result was not seen in *VTC4*- or *IMPL1*-deficient plants. Although we could not measure the endogenous level of *myo*-inositol in the *impl2* mutant because of its lethality, we assumed that it was not significantly reduced. Presumably, this was because VTC4 can compensate for the *impl2* mutation. In addition, exogenous *myo*-inositol did not rescue the *impl2* mutant phenotype and allow the isolation of homozygous plants (data not shown). Therefore, it is unlikely that the phenotype caused by homozygous *impl2* was due to a deficiency in IMP enzymatic activity.

IMPs belong to the phosphomonoesterase protein family, which is inhibited by Li^+. Alignment of IMP amino acids indicates that there is a well-conserved "A" motif containing a putative substrate recognition site and a glutamic acid residue responsible for Li^+ sensitivity (Neuwald et al. 1991; Bone et al. 1992; Atack et al. 1995; York et al. 1995; Gill et al. 2005). Human IMP and VTC4 have two enzyme activities, and an IMP from *Methanoccocus jannaschii* MJ0109 has fructose-1,6-bisphosphatase activity (Table 3; Stec et al. 2000). These results suggest that there are some enzymes with an A motif that have low substrate specificity. *Arabidopsis* IMPL1, IMPL2, and VTC4 also conserve A motif, indicating that these proteins may have enzymatic

activity like IMP, but *in vitro* some IMPs produce other sugar-monophosphates in addition to *myo*-inositol 3-phosphate.

In this study, we showed that *impl2* was partially rescued by exogenous addition of histidine. The efficiency of the rescue may depend on the growth conditions and plant vigor as suggested by Muralla et al. (2007). As the IMPL2 primary amino acid sequence exhibited significant similarity to that of L-histidinol-phosphate phosphatase, we tried to examine the different preferences in substrates between VTC4 and IMPL2 *in vitro*. We could not, however, obtain the IMPL2 protein produced in *Escherichia coli* in an active form. Independently, Petersen et al. (2010) reported direct evidence indicating that IMPL2 has L-histidinol-phosphate phosphatase activity, supporting our hypothesis.

The real-time PCR analysis of the genes for the *de novo* and salvage pathways of *myo*-inositol synthesis demonstrated that these genes were coordinately expressed in the vegetative and reproductive organs (Figs. 2, 4). *MIPS3* expression was highest in the root, unlike the other genes, and the biological significance of this increased expression is unclear at present. The observation that the time course of *IMP* expression during seed development was similar to that of *SAL1*, a gene for the enzyme in the salvage pathway of *myo*-inositol biosynthesis, suggests that the salvage pathway may also be involved in *myo*-inositol synthesis during seed development. The *MIPS1* transcript level in seed development was high from 4 to

12 DAF (Fig. 4), suggesting that *myo*-inositol 3-phosphate might be converted in the phytic acid pathway (Mitsuhashi et al. 2008; Abid et al. 2009). In conclusion, the gene expression patterns of *VTC4*, *IMPL1*, and *IMPL2* were similar but not identical quantitatively and spatiotemporally. Thus, further detailed studies including metabolomic analysis will be required.

Acknowledgements

We sincerely thank the following individuals for providing helpful advice and technical assistance: Dr. Takeshi Kuroha from the Department of Biology, University of Washington, Seattle, USA; Dr. Eiichi Minami from the Division of Plant Sciences, National Institute of Agrobiological Sciences, Tsukuba, Japan; Haniyeh Bidadi from the University of Tsukuba, Tsukuba, Japan for technical assistance; and the Arabidopsis Biological Resource Center for providing seeds of the T-DNA insertion lines.

This work was supported in part by Grant-in-Aid for Science Research on Priority Areas [Grant No. 21027004].

References

Abid G, Silue S, Muhovski Y, Jacquemin JM, Toussaint A, Baudoin JP (2009) Role of *myo*-inositol phosphate synthase and sucrose synthase genes in plant seed development. Gene 439:1–10

Atack JR, Broughton HB, Pollack SJ (1995) Structure and mechanism of inositol monophosphatase. FEBS Lett 361:1–7

Bone R, Springer JP, Atack JR (1992) Structure of inositol monophosphatase, the putative target of lithium therapy. Proc Natl Acad Sci USA 89:10031–10035

Clough SJ, Bent AF (1998) Floral dip: a simplified method for *Agrobacterium*-mediated transformation of *Arabidopsis thaliana*. Plant J 16:735–743

Conklin PL, Gatzek S, Wheeler GL, Dowdle J, Raymond MJ, Rolinski S, Isupov M, Littlechild JA, Smirnoff N (2006) *Arabidopsis thaliana VTC4* encodes L-Galactose-1-P phosphatase, a plant ascorbic acid biosynthetic enzyme. J Biol Chem 281:15662–15670

Diehl RE, Whiting P, Potter J, Gee N, Ragan CI, Linemeyer D, Schoepfer R, Bennett C, Dixon RAF (1990) Cloning and expression of bovine brain inositol monophosphatase. J Biol Chem 265:5946–5949

Fu J, Peterson K, Guttieri M, Souza E, Raboy V (2008) Barley (*Hordeum vulgare* L.) inositol monophosphatase: gene structure and enzyme characteristics. Plant Mol Biol 67:629–642

Gee NS, Ragan CI, Watling KJ, Aspley S, Jackson RG, Reid GG, Gani D, Shute JK (1988) The purification and properties of *myo*-inositol monophosphatase from bovine brain. Biochem J 249:883–889

Gill R, Mohammed F, Badyal R, Coates L, Erskine P, Thompson D, Cooper J, Gore M, Wood S (2005) High-resolution structure of *myo*-inositol monophosphatase, the putative target of lithium therapy. Acta Cryst D61:545–555

Gillaspy GE, Keddie JS, Oda K, Gruissem W (1995) Plant inositol monophosphatase is a lithium-sensitive enzyme encoded by a multigene family. Plant Cell 7:2175–2185

Hajdukiewicz P, Svab Z, Maliga P (1994) The small, versatile *pPZP* family of *Agrobacterium* binary vectors for plant transformation. Plant Mol Biol 25:989–994

Hallcher LM, Sherman WR (1980) The effects of lithium ion and other agents on the activity of *myo*-inositol-1-phosphatase from bovine brain. J Biol Chem 255:10896–10901

Islas-Flores I, Villanueva MA (2007) Inositol-1 (or 4)-monophosphatase from *Glycine max* embryo axes is a phosphatase with broad substrate specificity that includes phytate dephosphorylation. Biochim Biophys Acta 1770:543–550

Jefferson RA, Kavanagh TA, Bevan MW (1987) GUS fusions: beta-glucuronidase as a sensitive and versatile gene fusion marker in higher plants. EMBO J 6:3901–3907

Keller R, Brearley CA, Trethewey RN, Muller-Rober B (1998) Reduced inositol content and altered morphology in transgenic potato plants inhibited for 1D-*myo*-inositol 3-phosphatesynthase. Plant J 16:403–410

Laing WA, Bulley S, Wright M, Cooney J, Jensen D, Barraclough D, MacRae E (2004) A highly

specific L-galactose-1-phosphate phosphatase on the path to ascorbate biosynthesis. Proc Natl Acad Sci USA 101:16976–16981

Loewus FA, Loewus MW (1983) *Myo*-inositol: its biosynthesis and metabolism. Ann Rev Plant Physiol 34:137–161

Loewus FA, Murthy PPN (2000) *Myo*-inositol metabolism in plants. Plant Sci 150:1–19

McAllister G, Whiting P, Hammond EA, Knowles MR, Atack JR, Bailey FJ, Maigetter R, Ragan CI (1992) cDNA cloning of human and rat brain *myo*-inositol monophosphatase. Expression and characterization of the human recombinant enzyme. Biochem J 284:749–754

Mitsuhashi N, Kondo M, Nakaune S, Ohnishi M, Hayashi M, Hara-Nishimura I, Richardson A, Fukaki H, Nishimura M, Mimura T (2008) Localization of *myo*-inositol-1-phosphate synthase to the endosperm in developing seeds of *Arabidopsis*. J Exp Bot 59:3069–3076

Mormann S, Lömker A, Rückert C, Gaigalat L, Tauch A, Pühler A, Kalinowski J (2006) Random mutagenesis in *Corynebacterium glutamicum* ATCC 13032 using an IS6100-based

transposon vector identified the last unknown gene in the histidine biosynthesis pathway. BMC Genomics 7:205

Muralla R, Sweeney C, Stepansky A, Leustek T, Meinke D (2007) Genetic dissection of histidine biosynthesis in *Arabidopsis*. Plant Physiol 144:890–903

Murashige T, Skoog F (1962) A revised medium for rapid growth and bioassays with tobacco tissue culture Physiol Plant 15:473–497

Neuwald AF, York JD, Majerus PW (1991) Diverse proteins homologous to inositol monophosphatase. FEBS Lett 294:16–18

Nunes ACS, Vianna GR, Cuneo F, Amaya-Farfán J, Capdeville G, Rech EL, Aragão FJL (2006) RNAi mediated silencing of the *myo*-inositol-1-phosphate synthase gene (*GmMIPS1*) in transgenic soybean inhibited seed development and reduced phytate content. Planta 224:125–132

Ohnishi T, Ohba H, Seo KC, Im J, Sato Y, Iwayama Y, Furuichi T, Chung SK, Yoshikawa T

(2007) Spatial expression patterns and biochemical properties distinguish a second *myo*-inositol monophosphatase IMPA2 from IMPA1. J Biol Chem 282:637–646

Petersen LN, Marineo S, Mandalà S, Davids F, Sewell BT, Ingle RA (2010) The missing link in plant histidine biosynthesis: arabidopsis myoinositol monophosphatase-like2 encodes a functional histidinol-phosphate phosphatase. Plant Physiol 152: 1186–1196

Quintero FJ, Garciadebias B, Rodriguez-Navarro A (1996) The *SAL1* gene of *Arabidopsis*, encoding an enzyme with 3'(2'), 5'-bisphosphate nucleotidase and inositol polyphosphate 1-phosphatase activities, increases salt tolerance in yeast. Plant Cell 8:529–537

Stec B, Yang H, Johnson KA, Chen L, Roberts MF (2000) MJ0109 is an enzyme that is both an inositol monophosphatase and the 'missing' archaeal fructose-1,6-bisphosphatase. Nat Struct Biol 7:1046–1050

Stepansky A, Leustek T (2006) Histidine biosynthesis in plants. Amino Acids 30:127–142

Styer JC, Keddie J, Spence J, Gillaspy GE (2004) Genomic organization and regulation of the

LeIMP-1 and *LeIMP*-2 genes encoding *myo*-inositol monophosphatase in tomato. Gene 326:35–41

Suzuki M, Tanaka K, Kuwano M, Yoshida KT (2007) Expression pattern of inositol phosphate-related enzymes in rice (*Oryza sativa* L.): implications for the phytic acid biosynthetic pathway. Gene 405:55–64

Takimoto K, Okada M, Matsuda Y, Nakagawa H (1985) Purification and properties of *myo*-inositol-1-phosphatase from rat brain. J Biochem 98:363–370

Torabinejad J, Donahue JL, Gunesekera BN, Allen-Daniels MJ, Gillaspy GE (2009) VTC4 is a bifunctional enzyme that affects myoinositol and ascorbate biosynthesis in plants. Plant Physiol 150:951–961

York JD, Ponder JW, Majerus PW (1995) Definition of a metal-dependent/Li^+-inhibited phosphomonoesterase protein family based upon a conserved three-dimensional core structure. Proc Natl Acad Sci USA 92:5149–5153

Figure Legends

Fig. 1 Histochemical staining of GUS activity in *pVTC4::GUS*, *pIMPL1::GUS*, and *pIMPL2::GUS* transgenic plants 5 (a, c, e) or 10 (b, d, f) d after sowing. Scale bars = 1 mm.

Fig. 2 Expression analysis of genes in the *IMP* (a) and *MIPS* family (b), as well as *SAL1* (b), using quantitative real-time PCR in different organs. Gene expression patterns were analyzed from cDNA templates of rosettes, roots, stems, and cauline leaves from plants 3 to 4 wk after sowing. For each gene, duplicate experiments were performed using different samples (indicated by black and gray bars).

Fig. 3 Histochemical staining of GUS activity during seed development. Early globular-stage embryos (a, d, g), late torpedo embryos (b, e, h), and flowers (c, f, i) of *pVTC4::GUS*, *pIMPL1::GUS*, and *pIMPL2::GUS* transgenic plants. Ep, embryo proper; En, endosperm; Pi, pistil. Scale bars = 0.1 mm (a, b, d, e, g, h), 0.5 mm (f, i), and 1 mm (c).

Fig. 4 Expression analysis of genes in the *IMP* (a) and *MIPS* family (b), as well as *SAL1* (b), using quantitative real-time PCR during seed development. Gene expression patterns were analyzed from cDNA templates of flower buds (FB) and siliques at 4, 8, and 12 DAF. For each

gene, duplicate experiments were performed using different samples (indicated by black and gray symbols).

Fig. 5 T-DNA insertion site in *IMPL2* (At4g39120) in the T-DNA insertion line SALK_076930. Gray boxes indicate exons. The PCR primers (LBb1) used to amplify the left border (LB) of the T-DNA are shown by black arrows. RB indicate right T-DNA border. Gray arrows represent At4g39120 gene-specific primers S1 and AS1. Primer sequences can be found in the Materials and methods.

Fig. 6 Phenotype of the seeds of self-pollinated *impl2* heterozygous plants and rescue with wild-type *IMPL2*. Morphology of the normal seeds from a wild-type silique (a), of seeds from self-pollinated *impl2* heterozygous plants (b), and of seeds from a complemented heterozygous *impl2* mutant using full-length *IMPL2* (e). All siliques were examined in the green mature seed stage after 7 DAF. The aborted seeds are marked by arrowheads. Microscopic observation of an aborted (left) and normal (right) embryo in a single silique from an *impl2* heterozygous plant 5 DAF (c). Screening of the gentamycin-resistant T_2 heterozygous plants, complemented with a full-length *IMPL2*, was verified by PCR (d). Primers S1/AS1, LBb1/AS1, and Gm-S1/Gm-AS1 were used to demonstrate the presence of *IMPL2*, the T-DNA insertion, and gentamicin

(Gm)-resistant genes, respectively. Scale bar = 1 mm (a, b, e) and 30 μm (c).

Fig. 1

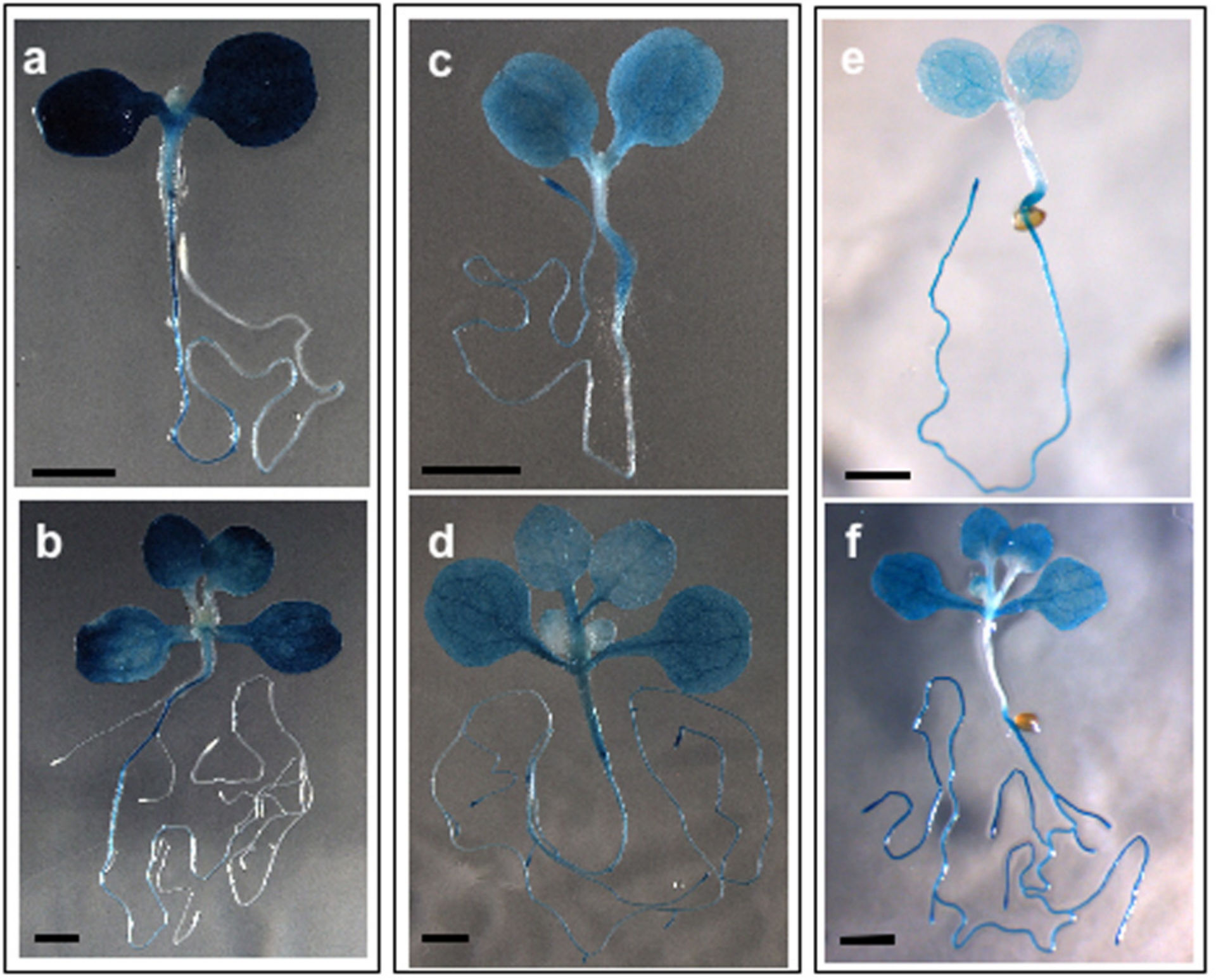

Fig. 2

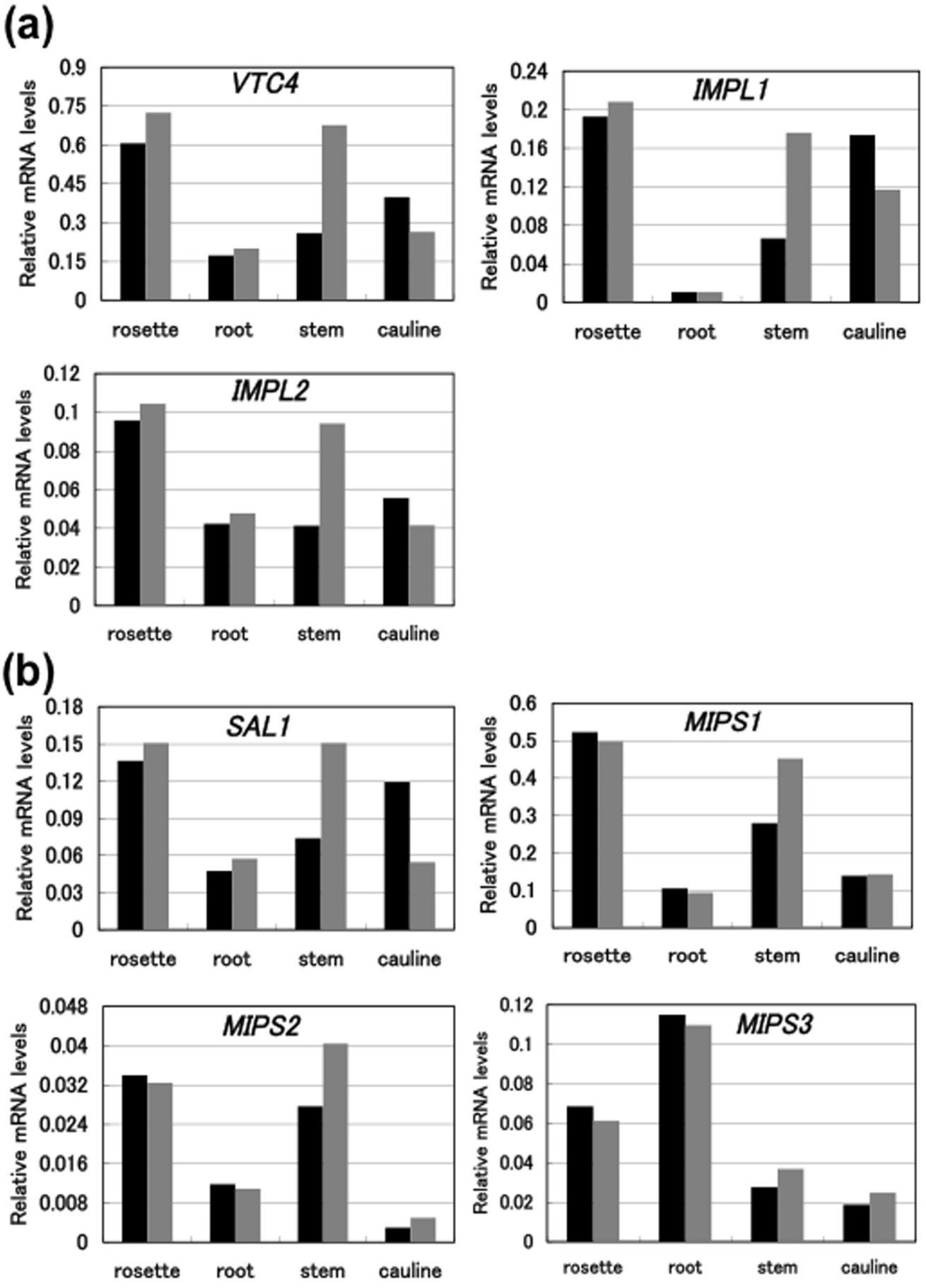
(a)
VTC4
Relative mRNA levels
0.9
0.75
0.6
0.45
0.3
0.15
0
rosette
root
stem
cauline
IMPL1
Relative mRNA levels
0.24
0.2
0.16
0.12
0.08
0.04
0
rosette
root
stem
cauline
IMPL2
Relative mRNA levels
0.12
0.1
0.08
0.06
0.04
0.02
0
rosette
root
stem
cauline
(b)
SAL1
Relative mRNA levels
0.18
0.15
0.12
0.09
0.06
0.03
0
rosette
root
stem
cauline
MIPS1
Relative mRNA levels
0.6
0.5
0.4
0.3
0.2
0.1
0
rosette
root
stem
cauline
MIPS2
Relative mRNA levels
0.048
0.04
0.032
0.024
0.016
0.008
0
rosette
root
stem
cauline
MIPS3
Relative mRNA levels
0.12
0.1
0.08
0.06
0.04
0.02
0
rosette
root
stem
cauline

Fig. 3

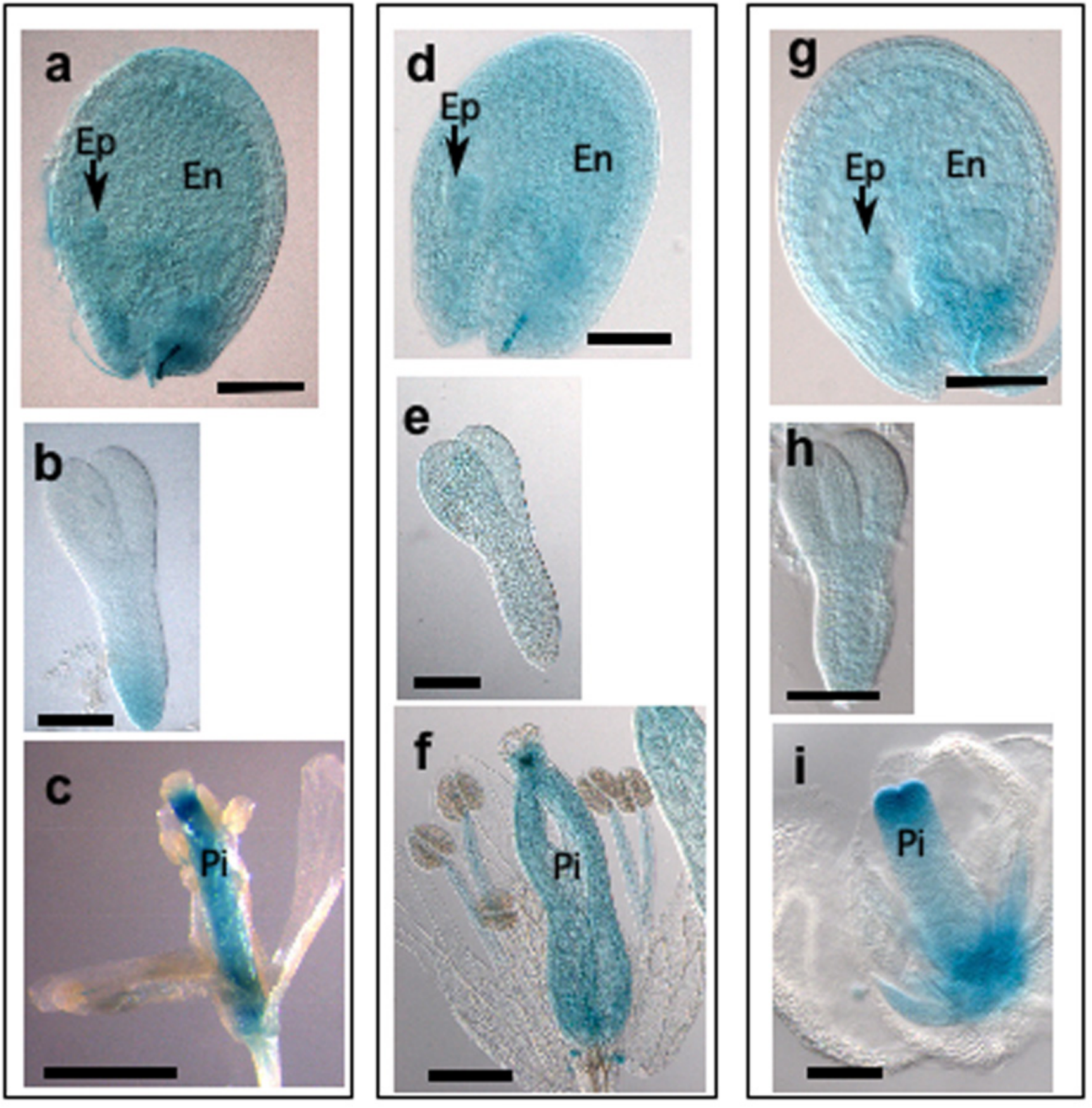
pVTC4::GUS
pIMPL1::GUS
pIMPL2::GUS
a
Ep
En
b
c
Pi
d
Ep
En
e
f
Pi
g
Ep
En
h
i
Pi

Fig. 4

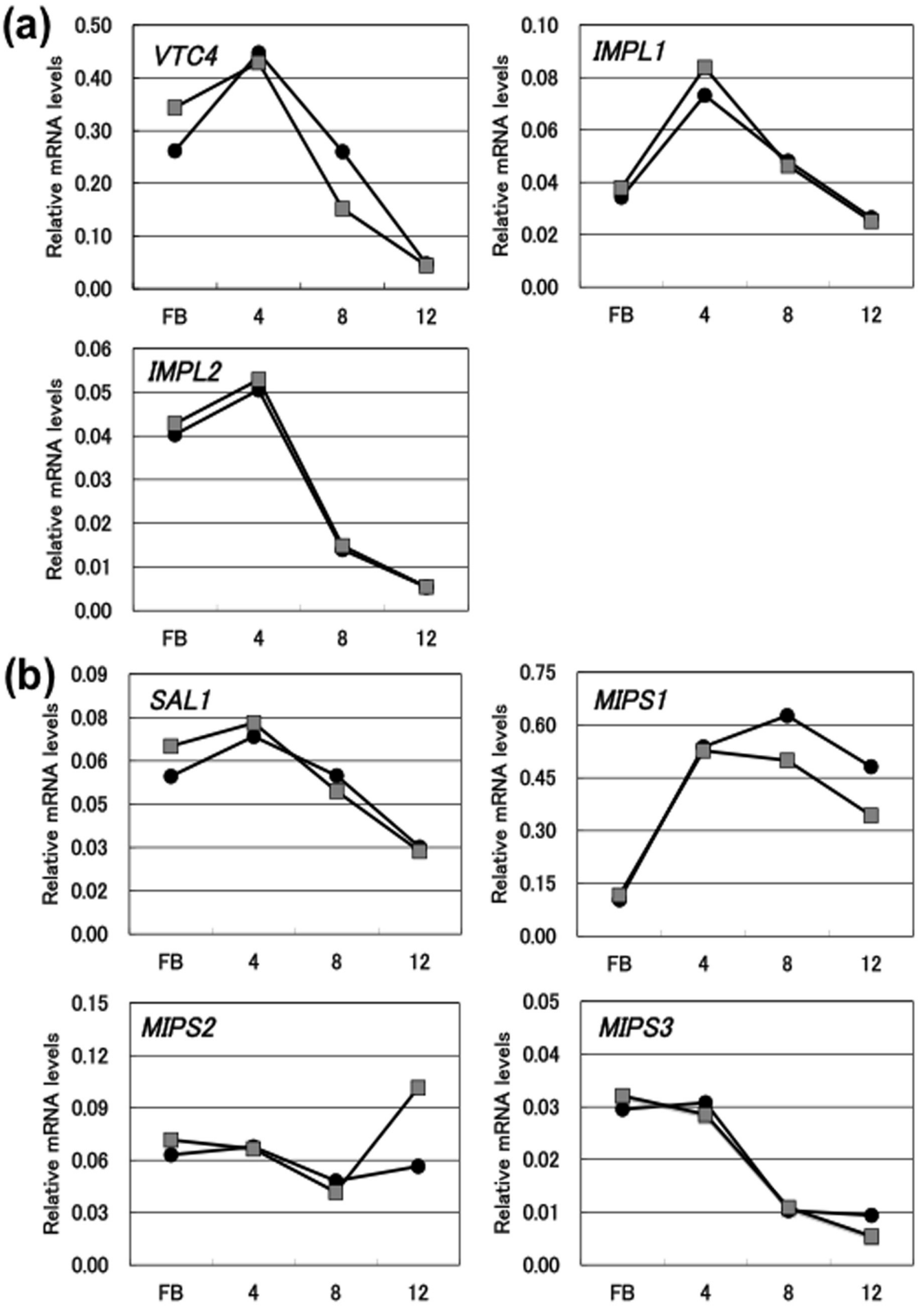
(a)
VTC4
IMPL1
IMPL2
(b)
SAL1
MIPS1
MIPS2
MIPS3
Relative mRNA levels
FB
4
8
12

Fig. 5

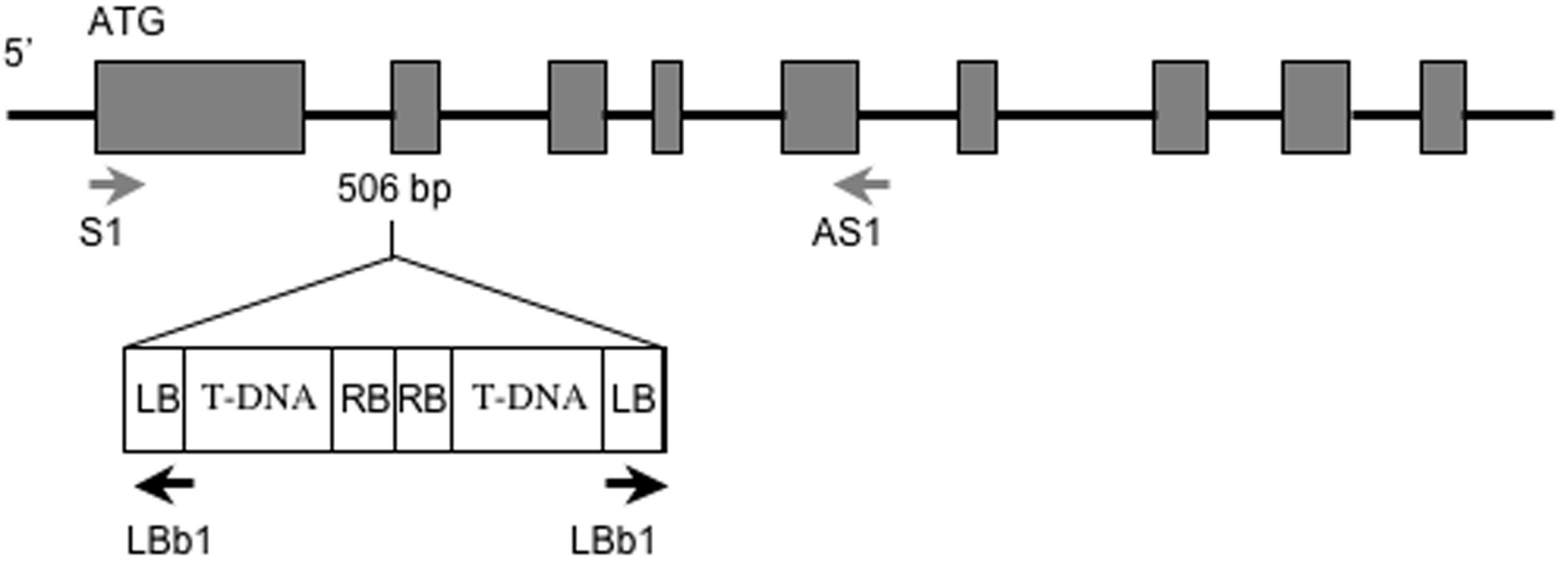

Fig. 6

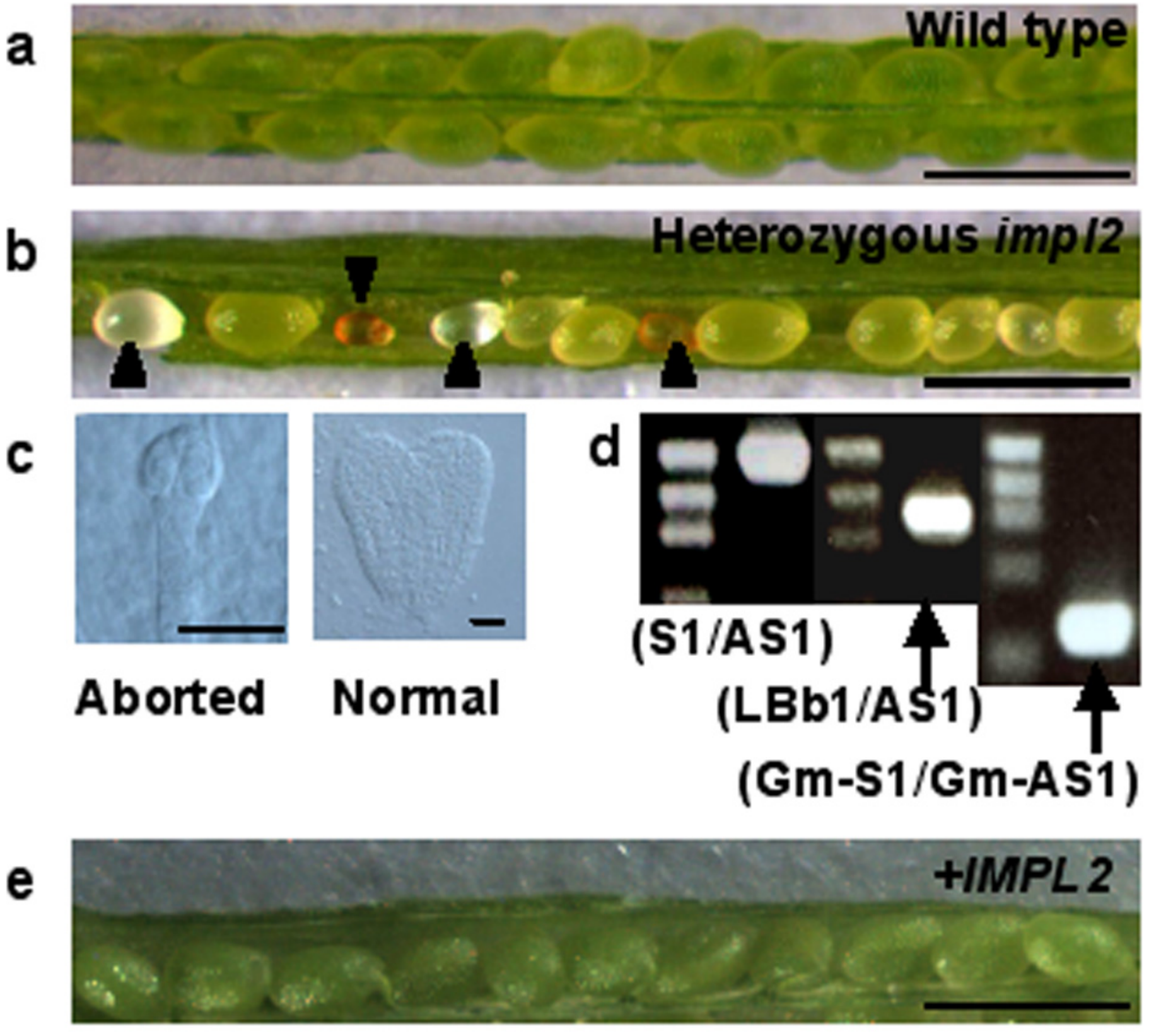
a
Wild type
b
Heterozygous impl2
c
Aborted
Normal
d
(S1/AS1)
(LBb1/AS1)
(Gm-S1/Gm-AS1)
e
+IMPL2

Table 1 Number of normal and aborted seeds in wild type, *impl2*, and *impl2 + IMPL2*

Allele	Siliques	Normal seeds	Aborted seeds	Total	Aborted seeds (%)	SD
impl2	12	358	115	473	24.3*	3.5
Wild type	12	369	6	375	1.6	1.4
impl2 + IMPL2	12	431	28	459	5.4*	3.9

SD, standard deviation

*Significant differences (P<0.01) between *impl2* and *impl2 +IMPL2* by paired t test analysis

Table 2 Number of normal and aborted seeds in wild-type plants and in plants heterozygous for *impl2*

Allele	Histidine	Siliques	Normal seeds	Aborted seeds	Total	Aborted seeds (%)	SD
Wild type	−	12	230	0	230	0.0	0.0
Wild type	+	12	269	9	278	2.8	2.8
Heterozygous	−	12	267	90	357	25.0*	2.8
Heterozygous	+	12	273	61	334	18.8*	2.1

SD: Standard Deviation

*Significant differences ($P<0.04$) between Heterozygous(-His) and Heterozygous(+His) by paired t test analysis

Four siliques from a primary flowering stem on each of three heterozygous plants were screened for aborted seeds after daily watering with or without 500 μM histidine.

Table 3 Bifunctional enzymes in the IMP family

Organism[a]	Enzyme	Enzyme activity		Amino acid sequence[b]
H. sapiens	IMPA1	IMPase, D-galactose 1-phosphatase	69	G**EE**SVAA-GEKSILTDNPT- **W**II--**DP**I**DG**TTNFVH -----
A. thaliana	VTC4	IMPase, L-galactose 1-phosphatase	70	G**EE**TTAAFGVTE-LTDEPT- **W**IV--**DP**L**DG**TTNFVH -----
A. thaliana	IMPL1	Putative IMPase	147	G**EE**GGIIG-DSSS--DYL-- **W**CI--**DP**L**DG**TTNFAH GYP--
A. thaliana	IMPL2	Putative IMPase	146	G**EE**KGWRCKEESA--DYV-- **W**VL--**DP**I**DG**TKSFIT GK---
M. jannaschii	MJ0109	IMPase, fructose-1,6-bisphosphatase	64	S**EE**LGVIDNSSE-------- **W**TVVI**DP**I**DG**SFNFIN GIPF-
				A motif

[a]*Homo sapiens* IMPA1 (NP005527), *Arabidopsis thaliana* VTC4 (NP186936), *A. thaliana* IMPL1 (NP564376), *A. thaliana* IMPL2 (NP195623), *Methanocaldococcus jannaschii* strain DSM2661 MJ0109 (NP247073)

[b]Amino acid sequence of a highly conserved region, including A motif. Identical residues are in boldface.

Underlined residues indicate the metal binding site of *Bos taurus* IMPA1 (Gill et al. 2005).